HSP90 inhibitor NVP-HSP990 alleviates rotavirus infection

Authors: Qingmin Zhu[1#], Yi Cao[2#], Xiaoping Wu[3], Zhunyi Xie[2], Yanyan Guo[2], Dongwei Meng[2], Xinyuan Zhou[2], Yuzhang Wu[2], Jintao Li[4,*], Haiyang He[4,*]

Affiliations:

[1] *Team 13 of the Fourth Brigade, Basic Medical School, Army Medical University (Third Military Medical University), Chongqing 400038, China*

[2] *Department of Immunology, Basic Medical School, Army Medical University (Third Military Medical University), Chongqing 400038, China*

[3] *Institute for Cancer Medicine and School of Basic Medical Sciences, Southwest Medical University, Luzhou, Sichuan 646000, China*

[4] *Department of Biosafety, Basic Medical School, Army Medical University (Third Military Medical University), Chongqing 400038, China*

*Corresponding author: Email: ljtqms@tmmu.edu.cn (J.L.); hehaiy@tmmu.edu.cn (H.H.);

[#] Qingmin, Zhu and Yi Cao have equal contributions to this study.

Abstract

Rotavirus (RV) infection is an important cause of hospitalization and even death of infants and young children, but conventional antiviral drugs such as nucleoside analogues as well as type I interferon are usually not included in treatment of RV diarrhea due to adverse side effects. Host heat shock protein 90 (HSP90) is commonly up-regulated and exploited by a series of viruses for successful infection including RV, rendering the possibility of small molecule HSP90 inhibitors as novel antiviral agents for control of RV infection. Here, we tested the effect of a novel HSP90 inhibitor NVP-HSP990 (HSP990), which possesses excellent oral bioavailability, on alleviating RV infection *in vitro* and *in vivo*. We found that HSP990 was low-cytotoxic and potently inhibited RV replication in MA104 and Caco-2 cells, though largely did not influence initial establishment of RV infection. Meanwhile, HSP990 also remarkably inhibited the activation of MAPK pathways induced by RV infection. HSP990 effectively alleviates RV diarrhea of BABL/c suckling mice, and remarkably inhibited RV replication as well as expressions of pro-inflammatory cytokines/chemokines in epithelial cells of intestinal mucosa. **IMPORTANCE** We revealed the novel HSP90

small molecule inhibitor HSP990 was a novel potent antiviral agent with low cytotoxity for the first time. HSP990 significantly inhibited RV replication *in vitro* and *in vivo* with low cytotoxicity and effectively alleviated RV diarrhea. These findings indicated that HSP990 could be a novel promising candidate of antiviral drug for RV infection.

[**Keywords]** Rotavirus; NVP-HSP990; Diarrhea; MAPK pathway

1. Introduction

Rotavirus (RV) infection is the main cause of diarrhea in infants and young children (1). According to the estimates of a latest global survey by WHO, RV causes about 0.64% hospitalizations and about 208,009 deaths of children less than 5 years of age in 28 low-income and middle-income countries (2). RV belongs to the family Reoviridae and is a membrane-less double-stranded RNA (dsRNA) virus with 11 segments of dsRNA encoding 12 viral proteins including 6 structural proteins (VP1~4, 6~7) and 6 non-structural proteins (NSP1~6) (3, 4). RV enters enterocytes under the mediation of membrane receptors such as integrins, takes off the outer capsid to form the double-layered particles (DLP) and starts genomic RNA transcription (5), which finally causes dysfunction of enterocytes and disorder of central nervous system, leading to severe dehydrating diarrhea and other clinic symptoms (6, 7).

Heat shock protein 90 (HSP90) is an atypical chaperone protein that exists in both eukaryotes and bacteria, and it has four isoforms: α, β, GRP94 and TRAP1 which are located in different sites in cells (8, 9). Many studies revealed that HSP90 is enrolled in viral infections, i.e., HSP90 promotes viral replication either by regulating cell signaling systems or by direct interacting with viral proteins such as Hepatitis B virus (Hepatitis B, HBV) reverse transcriptase (10), Hepatitis C virus non-structural protein 5A (NS5A) (11), and Influenza virus A RNA-dependent RNA polymerase (12). In RV infection, HSP90 on cell surface participates in RV entry into some tumor cell lines including U937, MCF-7, and Reh cells (13-15); meanwhile, it was also reported that

HSP90 contributes to RV replication *in vitro* (16, 17).

Small molecule inhibitors of HSP90 are recently popular and are pursued as a potential strategy for treatments of tumors and viral infections (18-21). However, till now there are few reports about the application of such HSP90 inhibitors in control of RV infection especially *in vivo*. NVP-HSP990 (HSP990) is a novel small molecule HSP90 inhibitor with a different structure from natural HSP90 inhibitor Geldanamycin (GA) and its derivative Tanespimycin (17-AAG) (22-24). HSP990 possesses high oral bioavailability and acts on the N terminal of both HSP90α and HSP90β with high binding affinity (25), indicating that it would probably possess promising application potential for control of viral infections, though there is no experimental data about the effect of HSP990 on virus control till now. Thus, in this study we aimed to evaluate the antiviral effect of HSP990 on RV infection *in vitro* and *in vivo*.

2. Materials and Methods

Cell culture, viral infection, and drug administration

MA104 cells were provided by Dr. Elschner (Friedrich-Loeffler-Institute). Caco-2 cells were from ATCC and kept in our institute. All the cells were cultured in Dulbecco's Modified Eagle Medium (DMEM) (Invitrogen) plus 10% (v/v) fetal bovine serum (FBS) (Gibco) at 37°C with 5% CO_2. RV Wa and SA11 strains were from the China Center for Disease Control and Prevention (Beijing, China) and propagated in MA104 cells. For RV infection, the viruses were diluted in DMEM, activated with 10 μg/ml trypsin (Amersco) for 30 min at 37°C, and then added to confluent target cells previously washed once with DMEM. After 1 h of incubation at 37°C, the inoculum was removed; the cells were then washed twice with DMEM and incubated with DMEM at 37°C till use. HSP90 inhibitors HSP990, GA, and 17-AAG (Selleck) were dissolved in DMSO and administrated with indicated concentrations *in vitro*, or orally administrated puls 90% (vol/vol) corn oil with indicated doses at 2 h p.i..

Virus preparation

RV-infected MA104 cells and their culture medium were freeze-thawed twice and centrifuged at 10,000 g for 20 min at 4°C for debris clearance. Supernatant of Wa strain was concentrated by centrifugation at 100,000 g with a SW28 rotor for 2 h at 4°C. For concentration of SA11 strain, NaCl was added to the supernatant of SA11 strain to a final concentration of 0.5 mol/L , then Polyethylene glycol (PEG, MW 6,000, Sangon Biotech) was added to a final concentration of 8% (w/v) with stirring overnight at 4°C, followed with centrifugation at 10,000 g for 2 h at 4°C. Both the virus pellets were suspended in TNC buffer (50 mmol/L Tris, 140 mmol/L NaCl, 10 mmol/L $CaCl_2$, pH 8.0) , filtered with 0.22 μm filters and subjected to sucrose density gradient centrifugation. Viruses were titrated and stored in aliquots at –70°C.

Cytotoxicity assay

To evaluate the cytotoxicity of different HSP90 inhibitors *in vivo*, 10000 Caco-2 or MA104 cells were seeded in 96-well plates and cultured for 12 h, then the indicated concentrations of HSP990, GA, or 17-AAG were added into the culture medium respectively, while a cell-free control was also set. 10 μl CCK-8 reagents (Beyotime) were added into each well 24 h after drug addition, and OD450 absorbance of each well was detected 3 h later using a Microplate Reader (Gene Company Limited). Relative cell viability rate = OD450 (drug-treated cells-cell free control) / OD450(0 μM drug-treated cells-cell free control). The 50 % cytotoxic concentration (CC50) was calculated by the GraphPad Prism 9.0 software.

Fluorescence foci assay (FFA)

FFA was carried out as described (26). Briefly, confluent monolayers of MA104 cells in 96-well tissue culture plates were infected with serially diluted (10^0, 10^1, 10^2, 10^3, and 10^4) supernatants containing infectious RV particles. At 20 h.p.i., the cells were fixed with 4% paraformaldehyde for 15 min, permeabilized with 1% Triton-X-100 for 7 min, quenched with 50 mM NH_4Cl for 10 min, and washed for 3 min in 0.01 M PBS twice. The cells were then incubated with FITC (fluorescein isothiocyanate)-

conjugated goat anti RV polyclonal Abs (Virostat, USA) (1:100) for 1 h at room temperature. The fluorescent foci-forming units (FFU) were counted under a fluorescent microscope (Olympus, Japan) with the help of a Visiolab semiautomatic system. Viral titer was expressed as FFU per milliliter.

In vitro inhibition of viral reproduction and cytopathic effect (CPE)

For analysis of the effects of different HSP990 inhibitors on RV reproduction *in vitro*, Caco-2 cells were infected with RV Wa or SA11 strains (MOI=1) and treated with indicated concentrations of HSP990, GA, or17-AAG. At 24 h p.i., the culture medium was collected and subjected to centrifugation at 1,000 g for 3 min. Then, the supernatant was subjected to analysis of viral load by FFA, and the 50% inhibiting concentration (IC50) of virus reproduction by each drug was calculated with the GraphPad Prism 9.0 software. For analysis of the effects of different HSP990 inhibitors on inhibition of CPE of RV infection *in vitro*, Caco-2 cells were infected with RV Wa or SA11 strains (MOI=3) and treated with the indicated concentrations of HSP990, GA, or17-AAG with equal dose of DMSO as positive control. At 72 h p.i., the positive control showed 100 % CPE under the microscope and the percentages of CPE in drug-treated groups were recorded. The IC50 of virus-induced CPE by the drugs was calculated by the GraphPad Prism 9.0 software.

Flow cytometric analysis

Caco-2 cells were infected with RV Wa strain (moi = 1), and at 20 h.p.i. the infected cells were digested with 0.25% trypsin-EDTA, the cells were fixed with 4% paraformaldehyde for 15 min, permeabilized with 1% Triton-X-100 for 7 min, quenched with 50 mM NH_4Cl for 10 min, and washed for 3 min in 0.01 M PBS twice. Cells were stained with FITC-labeled goat anti-rotavirus polyclonal antibody (1:100) for1 h at room temperature, and the frequency of infected cells was analysed with BD Canton II flow cytometry (BD).

qPCR analysis

RV-infected Caco-2 cells or epithelial cells of intestines form RV-infected suckling

146 mice were lysed in Trizol (Life Technologies) for RNA extraction and RNA was
147 further purified using RNeasy Plus Micro or Mini Kit (Qiagen). RNA was reverse
148 transcribed Using HiScript® II Q RT SuperMix for qPCR (+gDNA wiper) Kit
149 (Vazyme), and qRT-PCR was performed using AceQ qPCR SYBR Green Master Mix
150 (Vazyme) and corresponding primers on a CFX96 Touch Real-Time System
151 (Bio-Rad). Primers used for amplifications are listed in Table 1, from which human
152 β-actin or mouse Hprt genes were selected as internal reference.

153 *Western blot*

154 Caco-2 and MA104 cells were infected with RV or mock infected with PBS at 80%
155 confluence and treated with indicated concentration of HSP990 at indicated time
156 points. The cells were lysed with RIPA Lysis Buffer (Beyotime) plus protease
157 inhibitor cocktail (Thermo) at 16 h p.i.. The cell lysates were collected in 1.5 ml EP
158 tubes, sonicated 5 times for 15 s at 80 watts on ice, clarified by centrifugation at
159 12,000 g 10 min at 4°C, subjected to precast 4-12% or 4-20% gels for SDS-PAGE
160 and then transferred to 0.22 μm PVDF membranes (Millipore). After blocking with 5%
161 defatted milk, the membranes were incubated with rabbit mAbs to MAPK
162 components (JNK (9252T, CST), Phospho-JNK (4668T, CST), p38(8690T, CST),
163 Phospho-p38 (4511T, CST), ERK(4695T, CST), and Phospho-ERK (4370T, CST)) or
164 goat pAbs to RV particles (0501, Virostat), or with mouse mAb to β-actin (GB15001,
165 Servicebio) as internal reference. Afterwards, the membranes were incubated with
166 horseradish peroxidase (HRP)-conjugated anti-rabbit (7074S, CST), anti-goat (A0181,
167 Beyotime), or anti-mouse (7076S, CST) IgG. Immunoreactive bands were visualized
168 by using enhanced chemiluminescence's substrate (BeyoECL Plus, Beyotime).

169 *RV diarrhea of suckling mouse model*

170 For induction of RV diarrhea of suckling mice, 1×10^6 FFU RV (SA11 strain) was
171 orally inoculated to 7-days-old BALB/c suckling mice weighing 2.5~4.8 g. Then, we
172 used a scoring system to evaluate fecal consistency and color as described (27): no
173 stool (0 point); brown formed stool (1 point); brown soft stool (2 points); yellow soft

stool (3 points); and yellow watery stool (4 points). Mice with scores of ≥ 2 meant diarrhea occurrence, while mice with scores of < 2 meant no diarrhea. Diarrhea scores of the infected suckling mice were examined every 24 h by examination of fecal material. All work based on this animal model was done according to the requirements of Third Military Medical University Animal Ethics Committee.

In vivo RV inhibition of HSP990

7-days-old BABL/c suckling mice were orally inoculated with 1×10^6 RV SA11 strain. At 2 h p.i., the mice were treated with indicated doses of HSP990, GA, or 17-AAG, and with equal amount of DMSO as control. The diarrhea scores and body weights were recorded at indicated time points. The IC50 of RV diarrhea occurrence or of diarrhea scores by HSP990 was calculated using the GraphPad Prism 9.0 software.

To test the effect of HSP990 on RV replications *in vivo*, the RV-infected suckling mice, which were treated with 1mg/Kg HSP990 or equal amount of DMSO as control, were sacrificed by CO_2 asphyxiation at16 h.p.i and intestines (including duodenum, jejunum, ileum, and colon) of the mice were longitudinally split and washed in 1 ml DMEM each by shaking for 30 s. Then, the tissues were cut into 0.5 cm segments, incubated in Hank's buffer containing 2.5 mM $EDTANa_2$ and 1 mM DTT at 37°C with rotation at 200 rpm for 30 min, filtered with 70 μm strainer. Then the epithelial cells were pelleted by centrifugation at 1200 rpm for 5 min and lysed in Trizol for qPCR analysis. On the other hand, the DMEM containing intestinal contents was further vortexed for 30 s and then centrifuged at 12000 rpm for 5 min, and the supernatant was collected for RV titration by FFA.

Statistical analysis

Data were presented as means ± s.e.m. Statistical analysis was performed with Prism 9.0 (GraphPad). Student's *t* test was used for comparisons between 2 groups. One-way analysis of variance (ANOVA) test was used for comparisons between multiple groups. Two-way ANOVA test was used for comparisons of grouped data. *P*

values < 0.05 were considered significant (*P < 0.05; **P < 0.01; ***P < 0.001; ****P < 0.0001); ns: not significant, P > 0.05.

3. Results

3.1 Antiviral activity of HSP990 in vitro

HSP990 is structurally different from the traditional HSP90 inhibitors GA and 17-AAG and is much smaller (Fig. 1A). Using CCK-8 analysis, we compared the cytotoxicity of these HSP990 inhibitors on human intestinal epithelial cell line Caco-2 as well as rhesus monkey embryo kidney cell line MA104 which are both susceptible to RV infection. It is obviously HSP990 showed much less cytotoxicity than GA and 17-AAG, with CC50 values of 86.55 μM to Caco-2 cells and 97.15 μM to MA104 cells, which were both about 10 times of those of GA or 17-AAG (Fig. 1B).

To test the anti-RV effect of HSP990 *in vitro*, Caco-2 and MA104 cells were infected with human rotavirus Wa strain or simian rotavirus SA11 strain with a multiplicity of infection (MOI) of 1 and cultured in DMEM containing a series of concentrations of HSP990 inhibitors for 24 h. As shown in Fig. 2A, HSP990 inhibited RV reproduction with IC50 values of 4.876 nM in Caco-2 cells and6.176 nM in MA104 cells, which were both far less than those of GA or 17-AAG (Fig. 2A). Meanwhile, the IC50 values of HSP990 on RV-induced CPE on both Caco-2 and MA104 cells were also much lower, about 10% of those of GA or 17-AAG (Fig. 2B).

To further validate the anti-RV effect of HSP990, Caco-2 cells were infected with RV Wa or SA11 strain with a series (1~5) of MOI and cultured in DMEM containing 100 nM HSP990 for 24 h. It is clearly shown HSP990 also significantly inhibited RV reproduction even with high MOIs (Fig. 3A). We then evaluated the anti-RV effects of HSP990 (100 nM) administrated at different time points of RV infection. The results indicated that administration of HSP990 at 0~4 h p.i. achieved excellent inhibitory effects, though administration of HSP990 at 8~12 h p.i. also significantly inhibited RV reproduction; to be noted, even if HSP990 was administrated only for 2 h before RV infection but absent after RV infection, RV reproduction was also significantly

inhibited (Fig. 3B).

3.2 HSP990 inhibited RV genomic RNA synthesis and viral protein expressions.

We wondered whether HSP990 influences the establishment of RV infection. To this end, Caco-2 and MA104 cells were treated with a series of concentrations of HSP990 for 2 h before RV infection and infected with RV Wa or SA11 strains (MOI=1), followed with incubation in DMEM without HSP990 addition. As is shown, the percentages of RV-infected cells were largely uninfluenced across different concentrations of HSP990 administrated before RV infection (Fig. 4A, B); however, viral antigen expressions seemed declined in cells pretreated high HSP990 groups (100~10000 nM) to some extents (Fig. 4C). This result suggested that HSP990 did not influence the establishment of RV infection, but probably influence the expression of viral proteins. Therefore, we evaluated viral antigen expressions by immunofluorescence. As expected, HSP990 remarkably inhibited the expression of viral antigens (Fig. 5A). qPCR analysis further revealed significant reduction of genomic RNA synthesis of RV capsid proteins like VP2 and VP6 in RV-infected Caco-2 cells cultured with HSP990 (Fig. 5B). Accordingly, expressions of RV capsid proteins VP6 and VP7 were remarkably reduced in RV-infected Caco-2 or MA104 cells treated with HSP990 (Fig. 5C).

3.3 HSP990 inhibited activation of MAPK pathways induced by RV infection.

MAPK pathways, which are mainly composed of JNK, p38, and ERK signals, usually play important roles in viral infections and host antiviral immunity (28, 29). In RV infection, MAPK pathways were reported to be activated and were critical for RV reproduction (17, 30, 31). Herein, we evaluated the effect of HSP990 on RV-induced activation of MAPK pathways. We found that HSP990 robustly inhibited the activation of JNK, p38, and ERK signals in RV-infected MA104 and Caco-2 cells (Fig. 6A). We further found that HSP990 inhibition of MAPK pathways was dose-dependent, i.e., 10 nM or less HSP990 showed no inhibitory effect while 100 nM or more HSP990 exhibited strong inhibitory effect on MAPK pathway activation

258 in RV infection (Fig. 6B). Moreover, HSP990 inhibition of MAPK pathways was also
259 time-dependent, i.e., HSP990 must be administrated immediately after RV infection
260 for successful inhibition, while HSP990 administration later than 0.5 h p.i. would fail
261 (Fig. 6C).

262 *3.4 HSP990 alleviated RV infection in suckling mice*

263 As HSP990 possessed potent anti-RV effect *in vitro* as proved above, we wondered
264 whether HSP990 was effective on control of RV diarrhea. To this end, 7-days-old
265 BALB/c suckling mice (with a body weight of 2.5~4.8 g) were infected with 1×10^6
266 FFU RV SA11 strain orally. Different doses of HSP990 and controls were
267 administrated orally at 2 h p.i., and diarrhea scores of the infected suckling mice were
268 evaluated everyday as described (17, 27). At 24 h p.i. (day 1), it was found that
269 average diarrhea scores reduced along increased dose of HSP990, and the reduction
270 was especially remarkable in doses of 100~1000 μg/Kg (Fig. 7A). HSP990 inhibited
271 the occurrence of RV diarrhea with an IC50 value of 142.3 μg/Kg, and the IC50 value
272 of HSP990 on diarrhea score was 135.5 μg/Kg (Fig. 7B, C). By continuous
273 monitoring, we found that treatment with 1mg/Kg HSP990 as well as GA or 17-AAG
274 restored body growth of RV-infected suckling mice (Fig. 7D), however, only HSP990
275 significantly alleviated RV diarrhea (Fig. 7E, F). Therefore, these results indicated that
276 HSP990 also possessed potent ability to alleviate RV diarrhea.

277 As HSP990 was competent in control of RV diarrhea as proved above, we further
278 wondered whether it also significantly inhibited RV replication *in vivo* as it did *in*
279 *vitro*. To this end, RV-infected BABL/c suckling mice were treated with 1 mg/Kg
280 HSP990 at 2 h p.i. with equal amount of DMSO as control. At 16 h p.i., infectious RV
281 in the contents of intestines (including duodenum, jejunum, ileum and colon) of
282 RV-infected mice was titrated. It was found that infectious RV in intestinal contents
283 were remarkably reduced in ileum and colon of mice treated with HSP990, though
284 there was no significant difference in duodenum and jejunum between
285 HSP990-treated and control mice (Fig. 7F). Moreover, transcription of RV capsid
286 protein VP6 was remarkably reduced in epithelial cells of all intestines from

287 HSP990-treated mice compared to control (Fig. 7G). Therefore, these results
288 indicated that HSP990 also competently inhibited RV replication *in vivo*.
289 Viral infection usually intrigued the expressions of proinflammatory cytokines and
290 chemokines (17, 32). To assess the effects of HSP990 on mRNA expression of
291 proinflammatory cytokines/chemokines in RV-infected mice, we collected epithelial
292 cells of all intestines from HSP990-treated and control-treated RV-infected mice for
293 qPCR analysis. The results showed that mRNA expressions of proinflammatory
294 cytokines such as interleukin-2 (IL-2), interleukin-6 (IL-6), interferon-γ (INF-γ), as
295 well as chemokines including monocyte chemotactic protein-1(MCP-1) and
296 macrophage inflammatory protein 1α (MIP-1α) were reduced to certain extents in
297 most intestines of HSP990-treated mice; meanwhile, the expression of interleukin-10
298 (IL-10), a common immune negative regulator in intestines (33), was also obviously
299 inhibited in intestines below duodenum in HSP990-treated mice (Fig. 8).

300 **4. Discussion**

301 Successful viral infection depends on effective exploitation of host life system, for
302 example, viruses usually have to exploit host transcription and/or translation
303 mechanisms for production of viral antigens and assembly of viral particles (34, 35).
304 In the meantime, in order to better survive and evade host immune response, viruses
305 have developed some unique mechanisms to remodel host cell life system (36). Heat
306 shock proteins (HSPs) are important host chaperones that regulate various host life
307 processes, such as correct folding of proteins, protein targeted-transport, and cell
308 survival (37). Cell stress caused by viral infection results in enhanced expression of
309 various heat shock proteins, including HSP40, HSP70, and HSP90 etc., and viral
310 replications have been shown to be directly or indirectly dependent on one or more of
311 these HSPs (38, 39). HSP90 has a specific set of client proteins which is associated
312 with the regulation of signal transduction pathways involved in cell cycle and survival,
313 thereby maintaining the homeostasis of the host internal environment (40, 41).
314 Various reports revealed that many viruses, including RV, require the participation of
315 HSP90 in the replication process, while gene knockdown of HSP90 expression or the

use of chemical inhibitors of HSP90 could significantly inhibit viral replications *in vitro* (10-12, 16, 42, 43). Therefore, it would be promising to develop novel broad-spectrum antiviral drugs by targeting HSP90, and because these drugs do not target specific viral antigens, they will be more stable in antiviral effect and are less affected by viral mutation.

Design of small molecule chemical drugs targeting HSP90 has been gaining more and more interests in drug research in recent decades (18). The initial designs of novel HSP90 inhibitors mainly referred to the mechanism of HSP90 natural inhibitor GA or Radicicol, which targets to the ATP pocket of N-terminal domain of HSP90 to block HSP90 ATPase activity. Among them, the representatives include GA derivatives such as 17-allylamino-17-demethoxygeldanamycin (17-AAG), 17-N, N-dimethylaminoethyl-17-methoxygeldanamycin (17-DMAG), 17-AAG hydroquinone hydrochloride (IPI-504) and the Radicicol derivatives NVPAUY922, AT13387, and Ganetespib; Recently, with the increasing understanding of HSP90 subtypes and the interactions between HSP90 and its client proteins, a series of novel HSP90 inhibitors have emerged, which selectively inhibit HSP90 subtypes or specifically block the interaction between HSP90 and client proteins, so as to improve their inhibitory effects and safety (44, 45).

HSP990 is a novel small molecule HSP90 inhibitor targeting the N terminals of both HSP90α and HSP90β with high oral bioavailability previously tested in treatment of tumors and Huntington's disease (25, 46). However, till now there is no report about the roles of HSP990 in control of viral infections, though recently an *in silico* study predicted that HSP990 might alleviate COVID-19 symptoms through anti-inflammatory effects on SARs-CoV-2-infected lung cells (47). Here, our data indicated that HSP990 potently inhibited RV infection *in vitro* with IC50 values less than 10 nM in different cell lines. HSP990 mainly blocked RV replication but not initial infection establishment, which meant that HSP990 did not disturb RV membrane attachment, entry, and disruption of outer capsid to yield DLP (the active transcriptional unit of RV) for the initiation of genomic transcription, but suppressed

345 RV genomic transcriptions and expressions of RV antigens. However, whether
346 HSP990 inhibits the activity of RV transcriptase or inhibits the construction of new
347 DLP, both of which lead to repaired RV genomic RNA transcription and viral protein
348 expression, remains to be further investigated. In fact, although host HSP90 is
349 important for RV replication (16, 17), the detail mechanism remains largely unclear.

350 Viral infection is usually companied with the modulation of host signal pathways
351 which are exploited by virus to remodel host cell life system for better viral
352 replication (48-50). It was reported that RV infection significantly induced the
353 activation of most MAPK pathways including JNK, p38, and ERK signals, among
354 which p38 and ERK signals were critical to RV replication *in vitro* while JNK signal
355 was also critical for host production of IFN-β to function antiviral innate immunity
356 (30, 31, 51, 52). Here, we revealed that 100 nM or more HSP990 robustly inhibited
357 the activation of JNK, p38, and ERK signals in RV-infected MA104 and Caco-2 cells,
358 while 10 nM or less HSP990 showed no inhibitory effect. Given that HSP990
359 inhibited RV reproduction *in vitro* with IC50 values less than 10 nM, it makes sense
360 that the inhibitory effect of HSP990 on RV reproduction was not dependent on
361 suppression of MAPK pathways. Moreover, HSP990 inhibition on activation of
362 MAPK pathways only occurred within 0.5 h p.i., indicating that effective MAPK
363 inhibition of HSP990 might be dependent of quick and potent suppression of RV
364 genomic transcription which generated abundant viral dsRNA that triggered the
365 activation of host signaling network.

366 Although the mechanism of RV diarrhea still remains controversial (53-58),
367 inhibiting RV replication *in vivo* is of key interest in control of RV infection anyway.
368 However, conventional antiviral drugs such as nucleoside analogues as well as type I
369 interferon are usually not included in treatment of RV diarrhea probably due to
370 adverse side effects (59, 60), thus symptomatic treatment is usually the main choice,
371 which sometimes leads to severity of RV infection and even mortality of RV-infected
372 infants and young children due to sustained RV infection. In this study we revealed
373 that HSP990 effectively alleviated RV diarrhea in BABL/c suckling mice. HSP990

inhibited RV replication and expressions of pro-inflammatory factors (IL-2, IL-6, and IFN-γ) and chemokines (MCP-1 and MIP-1α) in epithelial cells of intestines from RV-infected suckling mice, indicating that HSP990 alleviated RV diarrhea probably by inhibiting the expression of viral antigens as well as RV-induced intestinal inflammation. To be noted, the immune negative regulator IL-10 was also repressed in HSP990 treatment, probably due to impaired RV antigen expression as well as low intestinal inflammation.

5. Conclusion

In this study we revealed HSP90 small molecule inhibitor HSP990 was a novel potent antiviral agent with low cytotoxity for the first time. HSP990 robustly blocked RV replication with low cytotoxicity *in vitro*, repressed RV-induced activation of MAPK pathways, effectively alleviated RV diarrhea, and inhibited expressions of pro-inflammatory cytokine/chemokines in intestinal epithelium of RV infected suckling mice. These findings indicated that HSP990 might be a novel promising candidate of antiviral drug for alleviating RV infection.

Declaration of Competing Interest

The authors declare that there are no conflicts of interest.

Acknowledgements

This work was supported by Chongqing Basic and Frontier Research Project (No. cstc2015jcyjBX0086) and National Natural Science Foundation of China (grant number 81570497 and 32070884).

References

1. Hasan H, Nasirudeen NA, Ruzlan MAF, Mohd Jamil MA, Ismail NAS, Wahab AA, Ali A. 2021. Acute Infectious Gastroenteritis: The Causative Agents, Omics-Based Detection of Antigens and Novel Biomarkers. Children (Basel) 8.
2. Cohen AL, Platts-Mills JA, Nakamura T, Operario DJ, Antoni S, Mwenda JM,

401 Weldegebriel G, Rey-Benito G, de Oliveira LH, Ortiz C, Daniels DS, Videbaek D,
402 Singh S, Njambe E, Sharifuzzaman M, Grabovac V, Nyambat B, Logronio J, Armah G,
403 Dennis FE, Seheri ML, Magagula N, Mphahlele J, Fumian TM, Maciel ITA, Gagliardi
404 Leite JP, Esona MD, Bowen MD, Samoilovich E, Semeiko G, Abraham D, Giri S,
405 Praharaj I, Kang G, Thomas S, Bines J, Liu N, Kyu HH, Doxey M, Rogawski McQuade
406 ET, McMurry TL, Liu J, Houpt ER, Tate JE, Parashar UD, Serhan F. 2022. Aetiology
407 and incidence of diarrhoea requiring hospitalisation in children under 5 years of age in
408 28 low-income and middle-income countries: findings from the Global Pediatric
409 Diarrhea Surveillance network. BMJ Glob Health 7.
410 3. Mathis PK, Ciarlet M, Campbell KM, Wang S, Owen KE, Ranheim TS. 2010.
411 Separation of rotavirus double-layered particles and triple-layered particles by
412 capillary zone electrophoresis. J Virol Methods 169:13-21.
413 4. Sadiq A, Bostan N, Yinda KC, Naseem S, Sattar S. 2018. Rotavirus: Genetics,
414 pathogenesis and vaccine advances. Rev Med Virol 28:e2003.
415 5. Long CP, McDonald SM. 2017. Rotavirus genome replication: Some assembly
416 required. PLoS Pathog 13:e1006242.
417 6. Hellysaz A, Hagbom M. 2021. Understanding the Central Nervous System Symptoms
418 of Rotavirus: A Qualitative Review. Viruses 13.
419 7. Lorrot M, Vasseur M. 2007. How do the rotavirus NSP4 and bacterial enterotoxins
420 lead differently to diarrhea? Virol J 4:31.
421 8. Hoter A, El-Sabban ME, Naim HY. 2018. The HSP90 Family: Structure, Regulation,
422 Function, and Implications in Health and Disease. Int J Mol Sci 19.

423 9. Powers MV, Workman P. 2006. Targeting of multiple signalling pathways by heat
424 shock protein 90 molecular chaperone inhibitors. Endocr Relat Cancer 13 Suppl
425 1:S125-35.
426 10. Hu J, Seeger C. 1996. Hsp90 is required for the activity of a hepatitis B virus reverse
427 transcriptase. Proc Natl Acad Sci U S A 93:1060-4.
428 11. Okamoto T, Nishimura Y, Ichimura T, Suzuki K, Miyamura T, Suzuki T, Moriishi K,
429 Matsuura Y. 2006. Hepatitis C virus RNA replication is regulated by FKBP8 and
430 Hsp90. EMBO J 25:5015-25.
431 12. Naito T, Momose F, Kawaguchi A, Nagata K. 2007. Involvement of Hsp90 in assembly
432 and nuclear import of influenza virus RNA polymerase subunits. J Virol 81:1339-49.
433 13. Rico J, Perez C, Hernandez J, Guerrero C, Acosta O. 2021. Cell surface heat shock
434 protein-mediated entry of tumor cell-adapted rotavirus into U-937 cells. Folia Microbiol
435 (Praha) 66:623-638.
436 14. Perez C, Rico J, Guerrero C, Acosta O. 2021. Role of heat-shock proteins in infection
437 of human adenocarcinoma cell line MCF-7 by tumor-adapted rotavirus isolates.
438 Colomb Med (Cali) 52:e2024196.
439 15. Rico J, Perez C, Guerrero R, Hernandez J, Guerrero C, Acosta O. 2020. Implication of
440 heat shock proteins in rotavirus entry into Reh cells. Acta Virol 64:433-450.
441 16. Dutta D, Bagchi P, Chatterjee A, Nayak MK, Mukherjee A, Chattopadhyay S,
442 Nagashima S, Kobayashi N, Komoto S, Taniguchi K, Chawla-Sarkar M. 2009. The
443 molecular chaperone heat shock protein-90 positively regulates rotavirus infectionx.
444 Virology 391:325-33.

445 17. Huang H, Liao D, Zhou G, Zhu Z, Cui Y, Pu R. 2020. Antiviral activities of resveratrol
446 against rotavirus in vitro and in vivo. Phytomedicine 77:153230.
447 18. Koren J, 3rd, Blagg BSJ. 2020. The Right Tool for the Job: An Overview of Hsp90
448 Inhibitors. Adv Exp Med Biol 1243:135-146.
449 19. Serwetnyk MA, Blagg BSJ. 2021. The disruption of protein-protein interactions with
450 co-chaperones and client substrates as a strategy towards Hsp90 inhibition. Acta
451 Pharm Sin B 11:1446-1468.
452 20. Solit DB, Chiosis G. 2008. Development and application of Hsp90 inhibitors. Drug
453 Discov Today 13:38-43.
454 21. Wang Y, Jin F, Wang R, Li F, Wu Y, Kitazato K, Wang Y. 2017. HSP90: a promising
455 broad-spectrum antiviral drug target. Arch Virol 162:3269-3282.
456 22. Gorska M, Popowska U, Sielicka-Dudzin A, Kuban-Jankowska A, Sawczuk W, Knap
457 N, Cicero G, Wozniak F. 2012. Geldanamycin and its derivatives as Hsp90 inhibitors.
458 Front Biosci (Landmark Ed) 17:2269-77.
459 23. Kim T, Keum G, Pae AN. 2013. Discovery and development of heat shock protein 90
460 inhibitors as anticancer agents: a review of patented potent geldanamycin derivatives.
461 Expert Opin Ther Pat 23:919-43.
462 24. McBride CM, Levine B, Xia Y, Bellamacina C, Machajewski T, Gao Z, Renhowe P,
463 Antonios-McCrea W, Barsanti P, Brinner K, Costales A, Doughan B, Lin X, Louie A,
464 McKenna M, Mendenhall K, Poon D, Rico A, Wang M, Williams TE, Abrams T, Fong S,
465 Hendrickson T, Lei D, Lin J, Menezes D, Pryer N, Taverna P, Xu Y, Zhou Y, Shafer
466 CM. 2014. Design, structure-activity relationship, and in vivo characterization of the

467 development candidate NVP-HSP990. J Med Chem 57:9124-9.

468 25. Menezes DL, Taverna P, Jensen MR, Abrams T, Stuart D, Yu GK, Duhl D,
469 Machajewski T, Sellers WR, Pryer NK, Gao Z. 2012. The novel oral Hsp90 inhibitor
470 NVP-HSP990 exhibits potent and broad-spectrum antitumor activities in vitro and in
471 vivo. Mol Cancer Ther 11:730-9.

472 26. He H, Mou Z, Li W, Fei L, Tang Y, Zhang J, Yan P, Chen Z, Yang X, Shen Z, Li J, Wu
473 Y. 2013. Proteomic methods reveal cyclophilin A function as a host restriction factor
474 against rotavirus infection. Proteomics 13:1121-32.

475 27. Boshuizen JA, Reimerink JH, Korteland-van Male AM, van Ham VJ, Koopmans MP,
476 Buller HA, Dekker J, Einerhand AW. 2003. Changes in small intestinal homeostasis,
477 morphology, and gene expression during rotavirus infection of infant mice. J Virol
478 77:13005-16.

479 28. Chander Y, Kumar R, Khandelwal N, Singh N, Shringi BN, Barua S, Kumar N. 2021.
480 Role of p38 mitogen-activated protein kinase signalling in virus replication and
481 potential for developing broad spectrum antiviral drugs. Rev Med Virol 31:1-16.

482 29. MacMicking JD. 2022. Rewiring the logic board of IFN signaling. Sci Signal
483 15:eadf0778.

484 30. Soliman M, Seo JY, Kim DS, Kim JY, Park JG, Alfajaro MM, Baek YB, Cho EH, Kwon
485 J, Choi JS, Kang MI, Park SI, Cho KO. 2018. Activation of PI3K, Akt, and ERK during
486 early rotavirus infection leads to V-ATPase-dependent endosomal acidification
487 required for uncoating. PLoS Pathog 14:e1006820.

488 31. Holloway G, Coulson BS. 2006. Rotavirus activates JNK and p38 signaling pathways

489 in intestinal cells, leading to AP-1-driven transcriptional responses and enhanced virus
490 replication. J Virol 80:10624-33.
491 32. Runfeng L, Yunlong H, Jicheng H, Weiqi P, Qinhai M, Yongxia S, Chufang L, Jin Z,
492 Zhenhua J, Haiming J, Kui Z, Shuxiang H, Jun D, Xiaobo L, Xiaotao H, Lin W,
493 Nanshan Z, Zifeng Y. 2020. Lianhuaqingwen exerts anti-viral and anti-inflammatory
494 activity against novel coronavirus (SARS-CoV-2). Pharmacol Res 156:104761.
495 33. Wei HX, Wang B, Li B. 2020. IL-10 and IL-22 in Mucosal Immunity: Driving Protection
496 and Pathology. Front Immunol 11:1315.
497 34. Anokhin B, Spearman P. 2022. Viral and Host Factors Regulating HIV-1 Envelope
498 Protein Trafficking and Particle Incorporation. Viruses 14.
499 35. Lawton JA, Estes MK, Prasad BV. 2000. Mechanism of genome transcription in
500 segmented dsRNA viruses. Adv Virus Res 55:185-229.
501 36. Strumillo ST, Kartavykh D, de Carvalho FF, Jr., Cruz NC, de Souza Teodoro AC,
502 Sobhie Diaz R, Curcio MF. 2021. Host-virus interaction and viral evasion. Cell Biol Int
503 45:1124-1147.
504 37. Kumar V, Roy S, Behera BK, Das BK. 2022. Heat Shock Proteins (Hsps) in Cellular
505 Homeostasis: A Promising Tool for Health Management in Crustacean Aquaculture.
506 Life (Basel) 12.
507 38. Bolhassani A, Agi E. 2019. Heat shock proteins in infection. Clin Chim Acta
508 498:90-100.
509 39. Zhang X, Yu W. 2022. Heat shock proteins and viral infection. Front Immunol
510 13:947789.

511 40. Schopf FH, Biebl MM, Buchner J. 2017. The HSP90 chaperone machinery. Nat Rev
512 Mol Cell Biol 18:345-360.
513 41. Farhan YAA, Arabdin M, Khan A. 2021. The Role of Heat Shock Proteins in Cellular
514 Homeostasis and Cell Survival. Cureus 13:e18316.
515 42. Evers DL, Chao CF, Zhang Z, Huang ES. 2012.
516 17-allylamino-17-(demethoxy)geldanamycin (17-AAG) is a potent and effective
517 inhibitor of human cytomegalovirus replication in primary fibroblast cells. Arch Virol
518 157:1971-4.
519 43. Wang C, Liu P, Luo J, Ding H, Gao Y, Sun L, Luo F, Liu X, He H. 2017. Geldanamycin
520 Reduces Acute Respiratory Distress Syndrome and Promotes the Survival of Mice
521 Infected with the Highly Virulent H5N1 Influenza Virus. Front Cell Infect Microbiol
522 7:267.
523 44. Costa T, Raghavendra NM, Penido C. 2020. Natural heat shock protein 90 inhibitors
524 in cancer and inflammation. Eur J Med Chem 189:112063.
525 45. Li L, Wang L, You QD, Xu XL. 2020. Heat Shock Protein 90 Inhibitors: An Update on
526 Achievements, Challenges, and Future Directions. J Med Chem 63:1798-1822.
527 46. Jackrel ME, Shorter J. 2011. Shock and awe: unleashing the heat shock response to
528 treat Huntington disease. J Clin Invest 121:2972-5.
529 47. Oh KK, Adnan M, Cho DH. 2021. Drug-repurposing against COVID-19 by targeting a
530 key signaling pathway: An in silico study. Med Hypotheses 155:110656.
531 48. Pleschka S. 2008. RNA viruses and the mitogenic Raf/MEK/ERK signal transduction
532 cascade. Biol Chem 389:1273-82.

533 49. Wu Y, Zhang Z, Li Y, Li Y. 2021. The Regulation of Integrated Stress Response
534 Signaling Pathway on Viral Infection and Viral Antagonism. Front Microbiol 12:814635.
535 50. Akbay B, Shmakova A, Vassetzky Y, Dokudovskaya S. 2020. Modulation of mTORC1
536 Signaling Pathway by HIV-1. Cells 9.
537 51. Jafri M, Donnelly B, McNeal M, Ward R, Tiao G. 2007. MAPK signaling contributes to
538 rotaviral-induced cholangiocyte injury and viral replication. Surgery 142:192-201.
539 52. He H, Zhou D, Fan W, Fu X, Zhang J, Shen Z, Li J, Li J, Wu Y. 2012. Cyclophilin A
540 inhibits rotavirus replication by facilitating host IFN-I production. Biochem Biophys Res
541 Commun 422:664-9.
542 53. Camilleri M, Nullens S, Nelsen T. 2012. Enteroendocrine and neuronal mechanisms in
543 pathophysiology of acute infectious diarrhea. Dig Dis Sci 57:19-27.
544 54. Guerrero CA, Acosta O. 2016. Inflammatory and oxidative stress in rotavirus infection.
545 World J Virol 5:38-62.
546 55. Gomez-Rial J, Rivero-Calle I, Salas A, Martinon-Torres F. 2020. Rotavirus and
547 autoimmunity. J Infect 81:183-189.
548 56. Belhorn T. 1999. Rotavirus diarrhea. Curr Probl Pediatr 29:198-207.
549 57. Ball JM, Tian P, Zeng CQ, Morris AP, Estes MK. 1996. Age-dependent diarrhea
550 induced by a rotaviral nonstructural glycoprotein. Science 272:101-4.
551 58. Hagbom M, Istrate C, Engblom D, Karlsson T, Rodriguez-Diaz J, Buesa J, Taylor JA,
552 Loitto VM, Magnusson KE, Ahlman H, Lundgren O, Svensson L. 2011. Rotavirus
553 stimulates release of serotonin (5-HT) from human enterochromaffin cells and
554 activates brain structures involved in nausea and vomiting. PLoS Pathog 7:e1002115.

555 59. Sun S, Lin X, Yang Y, Cen J, Luo F, Chen X. 2020. Acupoint application for rotavirus
556 diarrhea in infants and children: A protocol for systematic review and meta analysis.
557 Medicine (Baltimore) 99:e22227.
558 60. Jiang L, Tang A, Song L, Tong Y, Fan H. 2023. Advances in the development of
559 antivirals for rotavirus infection. Front Immunol 14:1041149.
560
561
562
563
564
565
566
567
568
569
570
571
572
573
574
575
576
577
578
579
580
581

582

583

584

585

586

587

588 **Figures and legends**

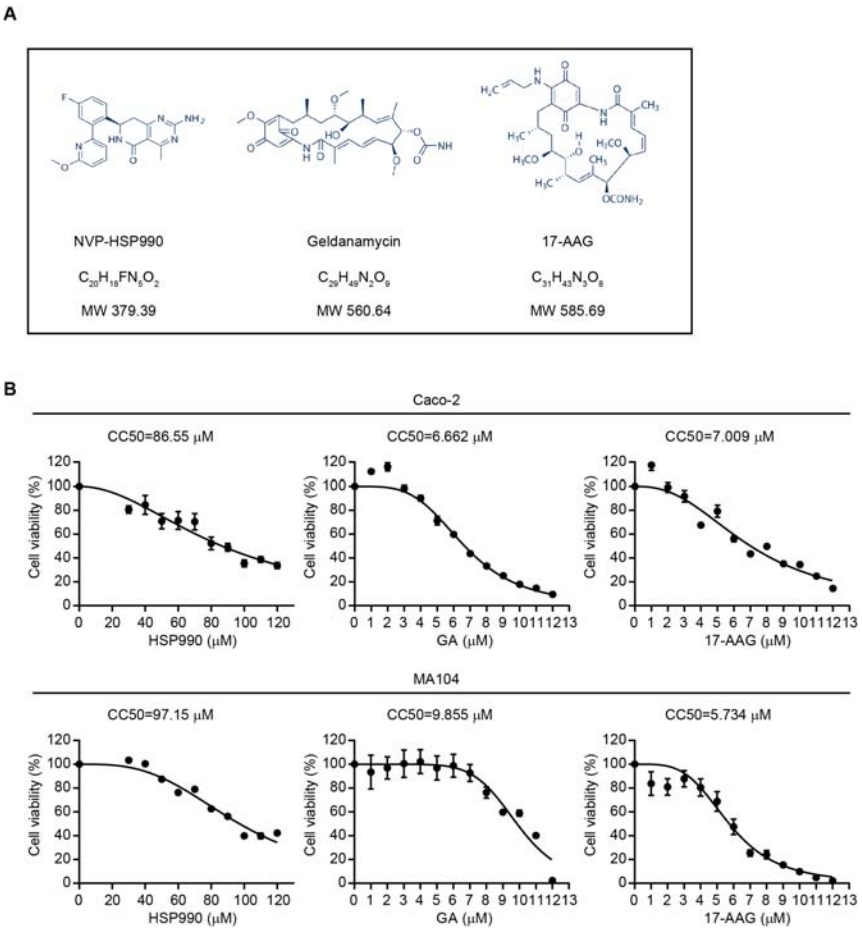

589

590 **Fig. 1. Cytotoxic effects of HSP990, GA, and 17-AAG on Caco-2 and MA104 cells.**
591 (A) Chemical structures of HSP990, GA, and 17-AAG. (B) Caco-2 or MA104 cells
592 were seeded in 96-well plates and cultured for 12 h, treated with different
593 concentrations of HSP990, GA, or17-AAG, and cell viability was evaluated by
594 CCK-8 24 h later. CC50 values of drugs were calculated by the GraphPad Prism 9.0
595 software. Data are presented as mean ± s.e.m. The experiments were performed in

596 triplicate and the data are representative of two independent experiments.

597

598

599

600

601

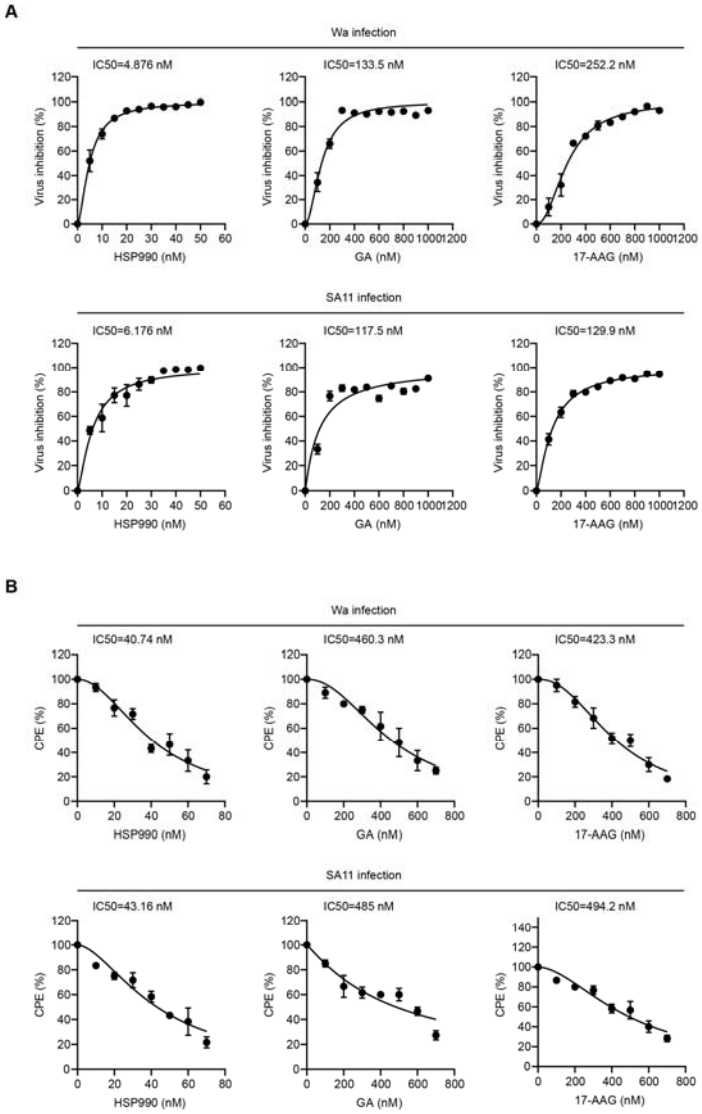

602

603 **Fig. 2. Antiviral activities of HSP990, GA, and 17-AAG.** (A) Caco-2 cells were
604 infected with RV Wa or SA11 strains (MOI=1) and treated with indicated
605 concentrations of HSP990, GA, or17-AAG. At 24 h p.i., viral titres in culture medium
606 were tested by FFA, and the IC50 value of each drug was calculated with the

607 GraphPad Prism 9.0 software. (B) Caco-2 cells were infected with RV Wa or SA11
608 strains (MOI=3) and treated with the indicated concentrations of HSP990, GA,
609 or17-AAG, and CPE were analysed at 72 h p.i.. The IC50 value of each drug was
610 calculated by the GraphPad Prism 9.0 software. The experiments were performed in
611 triplicate and the data are representative of two independent experiments.

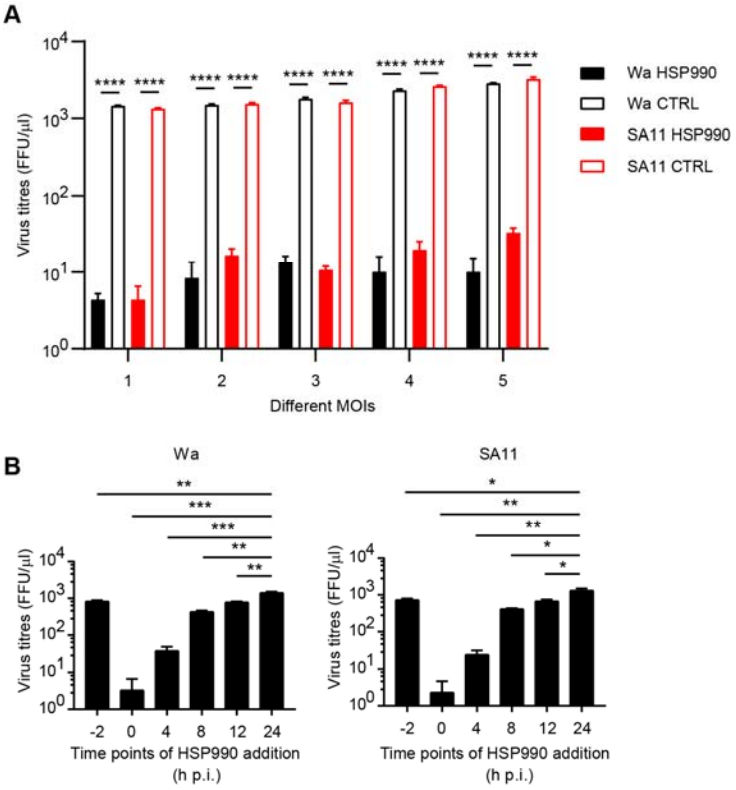

612

613 **Fig. 3. The influences of different MOIs and different time points of drug**
614 **administration on RV inhibition effect of HSP990.** (A) Caco-2 cells were infected
615 with different MOIs (1~5) of RV Wa or SA11 strains, and cultivated with DMEM
616 containing 100 nM HSP990 after viral infection for 24 h, then the supernatant was
617 harvested for virus titration with FFA. (B) Caco-2 cells were infected with RV Wa or
618 SA11 strains (MOI=1). The cells were treated with 100 nM HSP990 for only 2 h
619 before RV infection or at 0, 4, 8, 12, 24 h p.i., and then the supernatant was harvested
620 for virus titration with FFA. Data are presented as mean ± s.e.m. The experiments
621 were performed in triplicate and the data are representative of two independent
622 experiments. *$P < 0.05$, **$P < 0.001$, ***$P < 0.001$, ****$P < 0.0001$ (Two-way

ANOVA test (A) and one-way ANOVA test (B)).

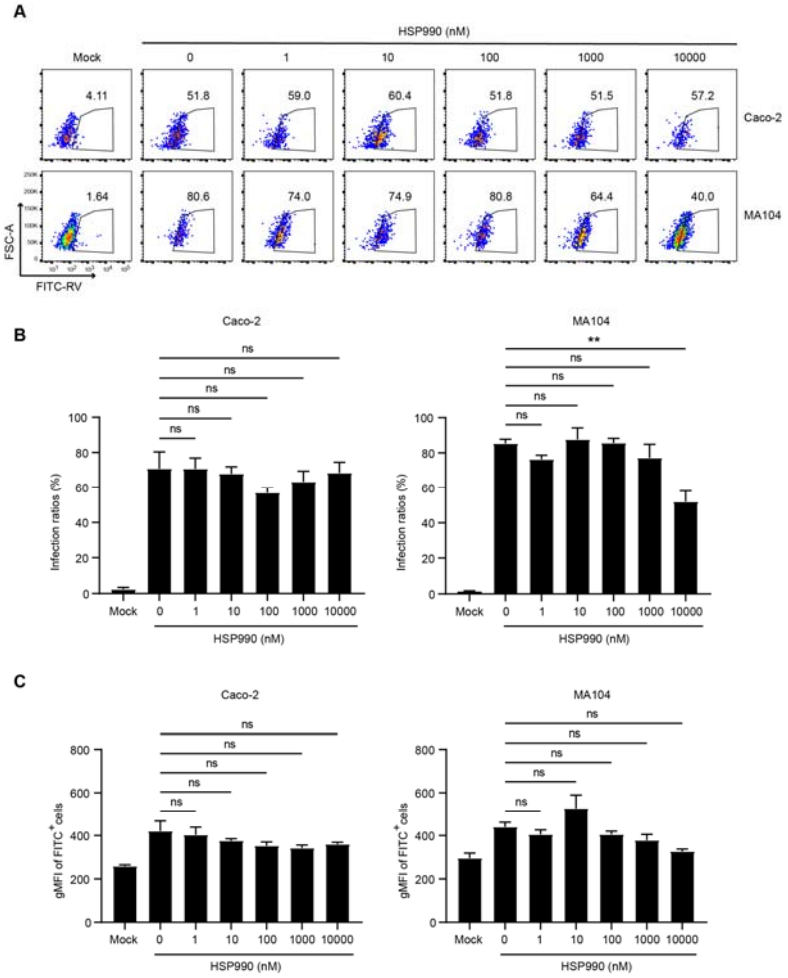

Fig. 4. HSP990 mainly did not influence the establishment of RV infections. Caco-2 and MA104 cells were treated with a series of HSP990 concentrations (0, 1, 10, 100, 1000, 10000 nM) for 2 h before RV Wa strain infection (MOI=1) respectively, and the cells were harvested at 20 h p.i. for FACS analysis of infection ratios and viral antigen expressions. Data are presented as mean ± s.e.m and are representative of three independent experiments. ns: no significance, $^{**}P < 0.001$ (one-way ANOVA

636 test).

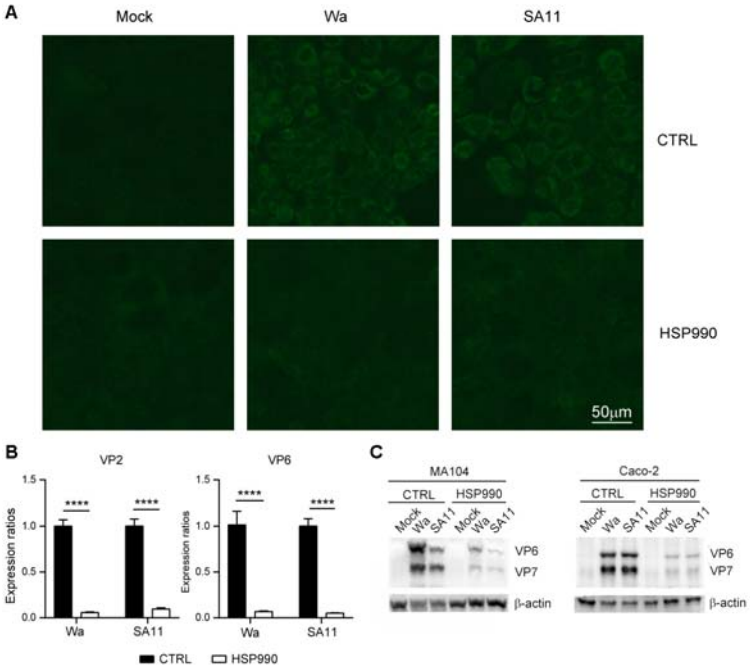

637

638 **Fig. 5. HSP990 inhibited expressions of RV antigens.** (A) Caco-2 cells growing on
639 coverslips were infected with RV Wa or SA11 strains (MOI=3), and cultivated with
640 DMEM containing 100 nM HSP990 after viral infection for 18 hours. Then the
641 infected cells were applied for IF analysis of expressions of RV antigens. (B, C)
642 Caco-2 cells were infected with RV Wa or SA11 strains (MOI=3), and cultivated with
643 DMEM containing 100 nM HSP990 after viral infection for 18 hours. Then the
644 infected cells were harvested for qPCR analysis (B) of replication of RV VP2 and
645 VP6 genes, or for WB analysis (C) of expressions of RV capsid proteins VP6 and VP7
646 with mock infection as negative control. Data are presented as mean ± s.e.m and are
647 representative of two independent experiments. ****$P < 0.0001$ (two-way ANOVA
648 test).

649

650

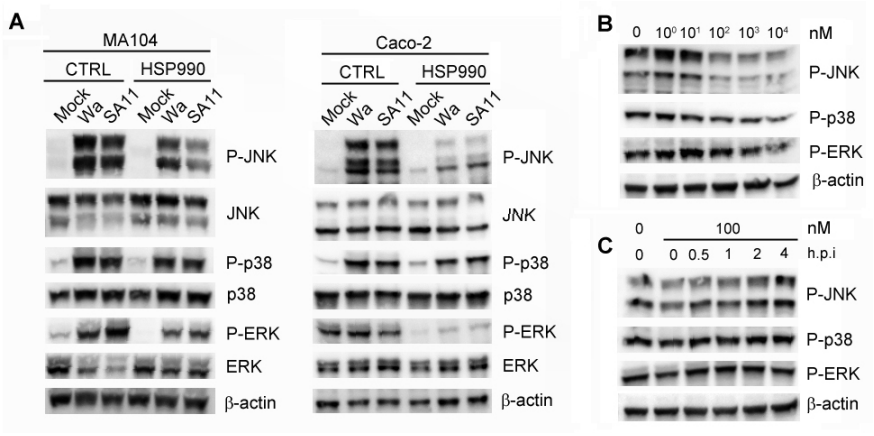

Fig. 6. HSP990 inhibited activation of MAPK pathways in RV infection. (A) MA104 and Caco-2 cells were infected with RV Wa or SA11 strains (MOI=1) or mock infected with PBS, and then cultivated with DMEM containing 100 nM HSP990 or equal amount of DMSO as control (CTRL) after viral infection for 20 h. Then the infected cells were harvested for WB analysis of expressions of MAPK components (JNK, Phospho-JNK (P-JNK), p38, Phospho-p38 (P-p38), ERK, and Phospho-ERK (P-ERK)) with β-actin as internal reference. (B) MA104 cells were infected with RV Wa strains (MOI=1) and cultivated with DMEM containing a series of HSP990 (0, 10^0, 10^1, 10^2, 10^3, 10^4 nM) concentrations after viral infection for 20 h. Then the infected cells were harvested for WB analysis of expressions of components MAPK pathways as above. (C) MA104 cells were infected with RV Wa strains (MOI=1), and treated with 100 nM HSP990 at 0, 0.5, 1, 2, 4 h p.i. or mock treated with equal amount of DMSO at 0 h p.i.. Then the infected cells were harvested for WB analysis of expressions of MAPK components at 20 h p.i. as above. Data are representative of two independent experiments.

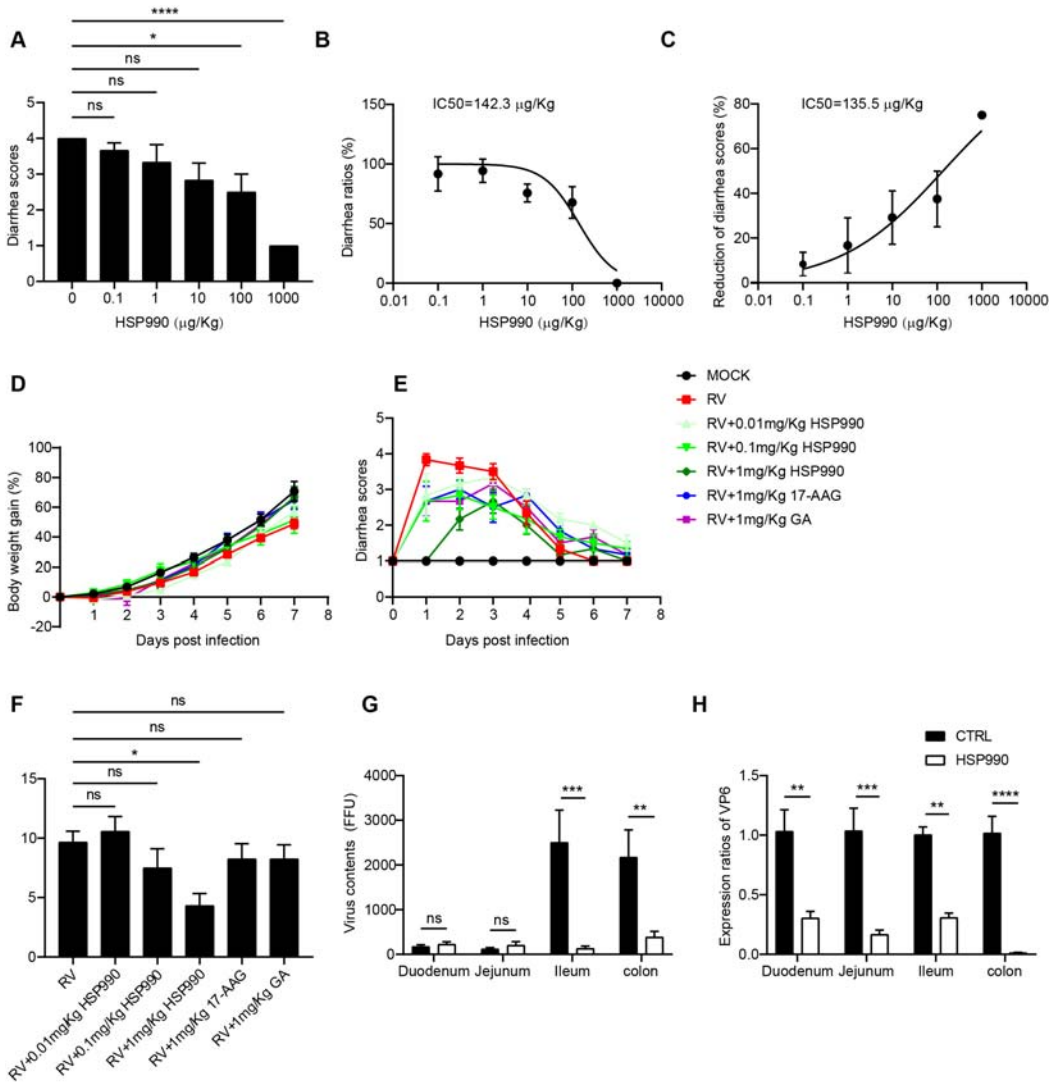

Fig.7. HSP990 inhibited rotavirus diarrhea in suckling mice. (A-C) 7-days old BABL/c suckling mice were orally invocated with 1×10^6 RV SA11 strain. At 2 h p.i., the mice were treated with a series dose (0.1, 1, 10, 100, 1000 μg/Kg) of HSP990. The effect of HSP990 on reduction of diarrhea scores of the RV-infected suckling mice at 24 h p.i. is shown (A), and the IC50 values of HSP990 to occurrence of RV diarrhea (B) or diarrhea scores (C) at 24 h p.i. were calculated by the GraphPad Prism 9.0 software. (D-F) 7-days old BABL/c suckling mice were orally invocated with 1×10^6 RV SA11 strain or mock infected with PBS. At 2 h p.i., the RV-infected suckling mice were treated with a series doses (0.01, 0.1, and 1mg/Kg) of HSP990, 1mg/Kg 17-AAG, or 1mg/Kg GA respectively, with equal dose of DMSO as control. Then

679 body weighs (D) and diarrhea scores (E) of the suckling mice were monitored from 0
680 to 7 days post infection, and the area under curve of diarrhea scores was assessed by
681 GraphPad Prism 9.0 software (F), while the curve of mock infection was set as
682 baseline. (G, H) 7-days old BABL/c suckling mice were orally invocated with 1×10^6
683 RV SA11 strain. At 2 h p.i., the RV-infected suckling mice were treated with 1mg/Kg
684 of HSP990 with equal dose of DMSO as control (CTRL). Then infectious viral
685 particles in contents of intestines of the mice were analyzed with FFA at 16 h p.i. (G),
686 and the gene expression of RV capsid protein VP6 in epithelial cells of intestines was
687 analysed with qPCR (H). Data are presented as mean ± s.e.m and are representative of
688 two independent experiments. ns: no significance, $*P < 0.05$, $**P < 0.001$, $***P <$
689 0.001, $****P < 0.0001$ (one-way ANOVA test (A, F) and two-way ANOVA test (G,
690 H)).
691
692
693
694
695
696
697
698
699
700
701

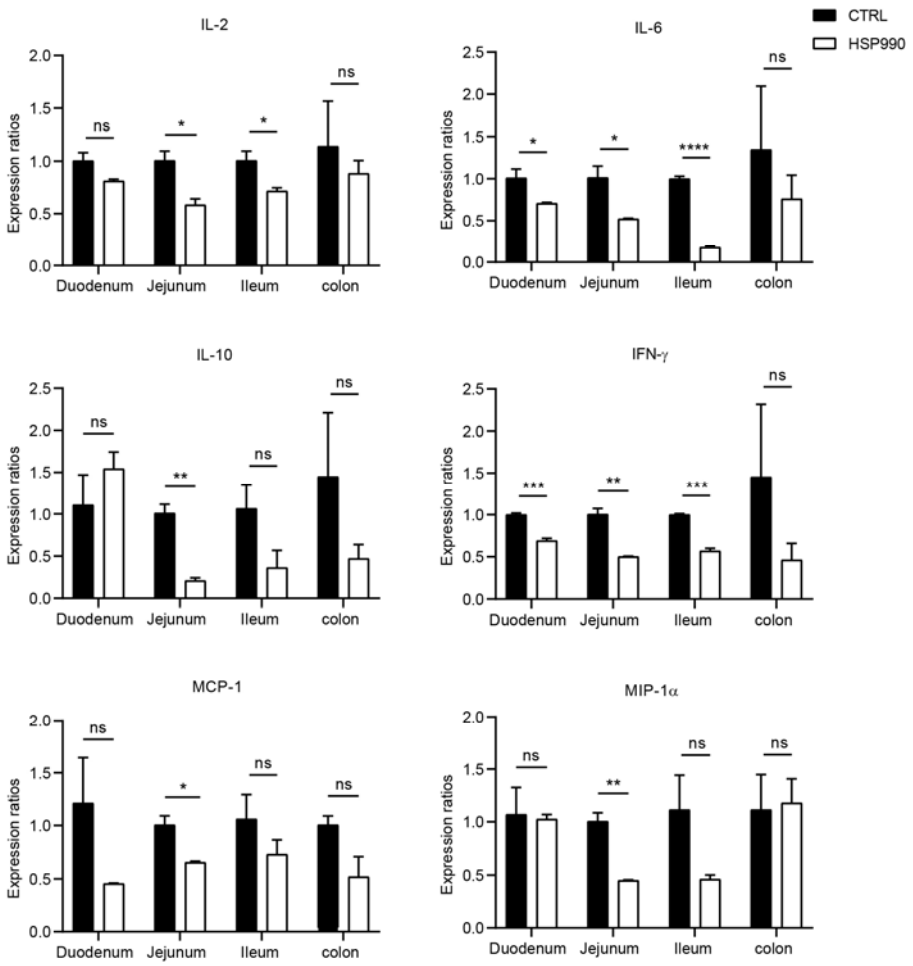

Fig.8. HSP990 reduced the expressions of intestinal pro-inflammatory cytokines/chemokines. 7-days-old BABL/c suckling mice were orally invocated with 1×10^6 RV SA11 strain. At 2 h p.i., the RV-infected suckling mice were treated with 1mg/Kg of HSP990 with equal dose of DMSO as control (CTRL). Then the gene expressions of six cytokines/chemokines including IL-2, IL-6, IL-10, INF-γ, MCP-1, and MIP-1α in the epithelial cells of intestines from the mice were analyzed with qPCR. Data are shown as mRNA ratios (folds) relative to CTRL. Data are presented as mean ± s.e.m and are representative of three independent experiments. ns: no significance, $*P < 0.05$, $**P < 0.001$, $***P < 0.001$, $****P < 0.0001$ (two-way ANOVA test).

715

716 Table 1. Primers used in qPCR analysis.

Primer name	Forward primer (5' – 3')	Reverse primer (5' – 3')
VP2	ttgcttgcgttcgtttcagc	tggggttggcgtttacagtt
VP6	tgctattaacgcaccagcca	aacctttccgcgtctggtag
IL-2	cggcatgttctggatttgac	tccaccacagttgctgactc
IL-6	ccggagaggagacttcacag	ttctgcaagtgcatcatcgt
IL-10	ccaagccttatcggaaatga	ttttcacaggggagaaatcg
IFN-γ	gcgtcattgaatcacacctg	tgagctcattgaatgcttgg
MCP-1	cactcacctgctgctactca	gcttggtgacaaaaactacagc
MIP-1α	gcaaccaagtcttctcagcg	ctcttagtcaggaaaatgacacc
Hprt	atcagtcaacgggggacata	cgagaggtccttttcaccag
β-actin	aatcgtgcgtgacatcaaag	ggattccatacccaagaagg

717

718